Whole Body Center of Mass Feedback in a Reflex-Based Neuromuscular Model Predicts Ankle Strategy During Perturbed Walking

A. Q. L. Keemink, T. J. H. Brug, E. H. F. van Asseldonk, A. R. Wu, and H. van der Kooij, *Member, IEEE*

***Abstract*— Active prosthetic and orthotic devices have the potential to increase quality of life for individuals with impaired mobility. However, more research into human-like control methods is needed to create seamless interaction between device and user. In forward simulations the reflex-based neuromuscular model (RNM) by Song and Geyer shows promising similarities with real human gait in unperturbed conditions. The goal of this work was to validate and, if needed, extend the RNM to reproduce human kinematics and kinetics during walking in unperturbed and perturbed conditions. The RNM was optimized to reproduce joint torque, calculated with inverse dynamics, from kinematic and force data of unperturbed and perturbed treadmill walking of able-bodied human subjects. Torques generated by the RNM matched closely with torques found from inverse dynamics analysis on human data for unperturbed walking. However, for perturbed walking the modulation of the ankle torque in the RNM was opposite to the modulation observed in humans. Therefore, the RNM was extended with a control module that activates and inhibits muscles around the ankle of the stance leg, based on changes in whole body center of mass velocity. The added module improves the ability of the RNM to replicate human ankle torque response in response to perturbations. This reflex-based neuromuscular model with whole body center of mass velocity feedback can reproduce gait kinetics of unperturbed and perturbed gait, and as such holds promise as a basis for advanced controllers of prosthetic and orthotic devices.**

***Index Terms*— Human gait, reflex modeling, neuromuscular control, prosthetics, orthotics.**

Manuscript received February 26, 2021; revised July 16, 2021; accepted August 11, 2021. Date of publication November 30, 2021; date of current version December 10, 2021. This work was supported in part by the EU Research Program FP7, FET-Proactive initiative "Symbiotic human-machine interaction" (ICT-2013-10) through the Project SYMBITRON under Project 611626, in part by the VICI Flexible Robotic Suit Project, and in part by the Netherlands Organisation for Scientific Research (NWO) under Grant 14429. *(A. Q. L. Keemink and T. J. H. Brug contributed equally to this work.) (Corresponding author: A. Q. L. Keemink.)*

This work involved human subjects or animals in its research. Approval of all ethical and experimental procedures and protocols was granted by the Local Ethics Committee (METC) under Approval No. NL50450.044.14.

A. Q. L. Keemink, E. H. F. van Asseldonk, and H. van der Kooij are with the Department of Biomechanical Engineering, University of Twente, 7522 NB Enschede, The Netherlands (e-mail: a.q.l.keemink@utwente.nl).

T. J. H. Brug is with the Department of Human Machine Teaming, Netherlands Organization for Applied Scientific Research (TNO), 2597 AK Den Haag, The Netherlands.

A. R. Wu is with the Department of Mechanical and Materials Engineering, Queen's University, Kingston, ON K7L 3N6, Canada.

Digital Object Identifier 10.1109/TNSRE.2021.3131366

I. Introduction

ACTIVE and portable prosthetic and orthotic (P/O) devices for the lower extremities have the potential to improve mobility and quality of life for individuals with reduced mobility [1], [2]. Effective control of an active P/O device requires understanding of human control of gait. Simulation studies have shown that control by neural feedback alone, provided by sensors and spinal reflexes, can generate human-like gait and can be made robust against pushes and variations in floor height. This was shown in a sagittal plane model by Geyer and Herr [3] and extended to 3D by Wang *et al.* [4], Geijtenbeek *et al.* [5] and extended with supraspinal high-level control contributions by Song and Geyer [6]. The latter model will be referred to as the reflex-based neuromuscular model (RNM).

A. The Original RNM

The original RNM [6] (schematically shown in top half of Fig. 1) requires different sources of information as input. First, supraspinal input: desired foot clearance height, foot placement location and it will choose which leg should be transferring to swing after double stance. Additionally, the RNM uses local sensory feedback from muscle stretch, muscle stretch rate, and muscle force, corresponding to signals traveling along type I and II afferents.

In addition to muscle state, also vestibular organs, joint proprioception and load receptors in the legs are modeled to calculate global body posture. The sensory signals are inputs for ten decentralized reflex control modules, representing ten groups of feedback loops, to generate muscle activation signals for eleven simulated Hill-type [7] muscles per leg. The resulting muscle forces act on the leg joints, resulting in net torques around those joints. Each leg has four joints that are actuated by this net muscle torque: hip ab-/adduction, hip flexion/extension, knee flexion/extension and ankle plantar-/dorsiflexion.

A total of 82 feedback parameters determine the behavior of the modeled spinal reflexes and supraspinal step location planning. The RNM can generate stable human-like gait in simulation for different scenarios, like walking up or down a slope, or on uneven terrain, and shows some balance robustness against low-force pushes without adjusting these parameters. This property is desirable for control methods of P/O devices to automatically adjust the gait pattern to different

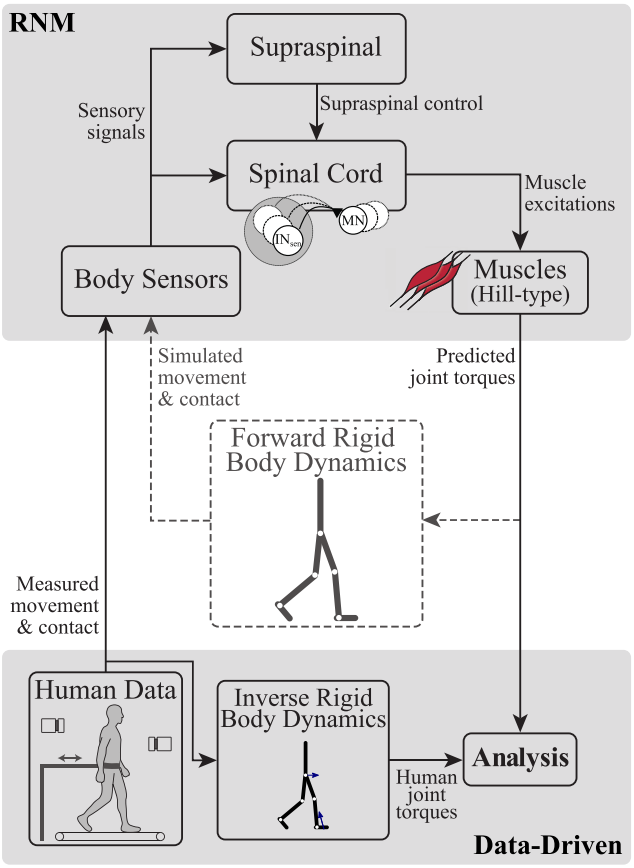

Fig. 1. Schematic overview of the original RNM (top shaded area and dashed lines) and the data-driven RNM (top and bottom shaded area). The dashed part has been removed and replaced with the bottom, data-driven, part. The data-driven model estimates joint torques using the recorded kinematics and ground-reaction forces as input. Parameters of the data-driven RNM are optimized to minimize the difference between the joint torques predicted by the RNM and the torques obtained from the data from inverse dynamics.

scenarios. Conventional control methods [8]–[16] based on fixed joint trajectories do not show this flexibility.

B. Using a RNM as a Controller

The possibility of the RNM to generate human-like adequate responses to perturbations is a strong motivation for developing such a model to be used in the control of P/O devices. In previous work [17]–[19] we showed that using a RNM as a controller for some of the joints in a robotic lower-extremity exoskeleton is a feasible control strategy.

However, using a RNM on its own has hardly any true walking stability guarantees due to possible mismatches in biomechanical parameters between the human-exoskeleton combination and the rigid body properties used in the model. Nonetheless, we have achieved promising results in our exoskeleton devices when some joints are position controlled while others are controlled by the RNM. In [19] walking speed of SCI patients was increased by such a controller. In [18] a RNM controller for an ankle exoskeleton resulted in improved gait for incomplete SCI patients. We have achieved stable exoskeleton walking with crutches by smoothly switching from fully RNM controlled joints to position control when leaving a safe, phase dependent, range of motion. The used position controller was limited to trajectory replay, so a controller that adapts foot placement based on body state could result in stable crutch-free walking where a RNM controls the joints for a vast majority of the movement time. Also, using a RNM as a joint-level controller shows greater flexibility and human like joint impedance, compared to trajectory control [20].

C. Contribution of This Work

This work delivers several novel contributions. We quantitatively investigate the model's ability to reproduce human joint torques during walking in unperturbed and perturbed conditions by having it imitate human torque data obtained from perturbed gait experiments. A qualitative comparison between human joint torques and model torques was done for the original RNM [6]. Additionally, in [21] a mostly qualitative comparison was made between model output and several disturbance experiments without improving model shortcomings. A quantitative analysis of torque responses to balance perturbations during walking is therefore lacking and is provided in this work. Moreover, both previous studies investigated the responses of a model that was optimized for metabolic energy efficiency, instead of optimizing it to imitate human responses. Consequently we show that the original model shows too high torque in the ankle joint and lacks capacity in the spinal reflex network to generate adequate torque responses in the ankle joint after perturbation. We therefore add a novel extension to the model that responds to whole body center of mass (CoM) information to be able to overcome this shortcoming.

To achieve the aforementioned goals, data from unperturbed and perturbed gait of able-bodied human subjects [22], [23] was used to drive the model, instead of using forward rigid body dynamics (as shown in the removed central part in Fig. 1). We optimized the parameters of these data-driven RNMs (DDRNM) by minimizing the difference between predicted joint torque from the model and joint torques obtained from able-bodied human gait data from inverse dynamics.

Using this data-driven approach, shortcomings in the model were found in modulating ankle torque in response to force perturbations at the pelvis in anteroposterior direction. These shortcomings were overcome with an additional control module reacting to changes in the velocity of the whole body CoM.

D. Outline of the Paper

This paper is structured as follows: Sec. II discusses the experimental paradigm behind the used data, the changes to the RNM, the used method for re-optimization and how the RNM was extended. Sec. III compares the output of the three model versions with human experimental data and each other. Sec. IV discusses the usefulness and limitations of the results and the physiological plausibility of the proposed model extension. Sec. V concludes the work.

II. Methods

Model torque data from three versions of the RNM was compared with able-bodied human torque data, obtained

through inverse dynamics methods, from experiments in which subjects were perturbed during treadmill walking. These three RNM versions were 1) the original model from [6] in data-driven form (Sec. II-B), 2) a re-optimized version of that same model (Sec. II-C) and 3) an extended & re-optimized version of that same model (Sec. II-D).

We will briefly summarize the used experimental procedures and analysis of the used data in Sec II-A, but for details we refer to Vlutters *et al.* [22], [23]. Subsequently the three model versions are explained.

A. Experimental Procedure

In the work of Vlutters *et al.* [22], [23] able-bodied subjects walked on a treadmill wearing a hip brace, wrapped tightly around the pelvis. The hip brace was connected via rods to motors to perturb the subject [SMH60, Moog, Nieuw-Vennep, The Netherlands] in anteroposterior (AP) direction or mediolateral (ML) direction by using indirect force control (admittance control) to provide a controlled perturbation force pulse. Kinematic data was collected using a 12 camera optical motion capture system [Visualeyez II, Phoenix Technologies, Burnaby, Canada]. Active LED marker frames were placed on the feet, lower legs, upper legs, front of the pelvis, sternum and head. Single LEDs were placed on the lateral malleoli and the lateral epicondyles of the femur. Perturbations to the subject were measured by FUTEK QLA131 load cells [FUTEK, Los Angeles, CA, USA] and ground reaction forces (GRF), for each foot separately, were measured by a dual-belt instrumented treadmill [custom Y- Mill, Motekforce Link, Culemborg, The Netherlands] at 1000 Hz. Subjects were perturbed at magnitudes of 4%, 8%, 12% and 16% of body weight (BW) in both AP or both ML directions. The perturbation was timed to occur directly after the right foot's toe-off, triggered by the vertical GRF of the right leg falling below a threshold. The duration of each perturbation was 150 ms. The walking speed was 4.5 km/h, scaled by the square-root of the leg-length [24].

OpenSIM v3.3 was used to perform inverse dynamics and inverse kinematics calculations on the marker and GRF data for all subjects separately. Marker and GRF data were both zero-phase low pass filtered at 20 Hz in MATLAB 2016b [Mathworks, Natick, USA], with the default 6 Hz low pass filtering of the inverse kinematics before calculating torques through inverse dynamics analysis. The default 23 DoF gait2354 model was used in OpenSIM, scaled to the subject's size with help of the marker data.

The used setup and experimental protocol for this experiment were approved by the local ethics committee (METC), approval number NL50450.044.14. All subjects gave prior written informed consent in accordance with the Declaration of Helsinki.

B. Original DDRNM

The RNM [6] was adapted to operate in an inverse dynamics fashion using experimental data as input: joint angles, angular velocities, information about stance or swing phase of each leg and the load on each leg. Signals were averaged over ten subjects and phase information was derived from the averaged data.

To determine the muscular torques from these inputs, forward dynamics calculations were required as the Hill-type muscle models and muscle-tendon dynamics need to be integrated to obtain the muscle length. A schematic overview can be found in the top part of Fig. 1. For fair comparisons, human torque (before averaging) and model torque were normalized to mgl [24], where m is the subject's body mass, l the subject's body length and g is the gravitational acceleration.

We used data of 16 strides out of the total experimental data, which were stitched together into a single dataset. For the perturbed cases, the perturbation amplitude increased each stride. The stitched dataset was as follows:

- four strides of unperturbed walking,
- four strides with backward perturbation (4%, 8%, 12%, 16% of BW),
- four strides with forward perturbation (4%, 8%, 12%, 16% of BW),
- four strides with outward perturbation (4%, 8%, 12%, 16% of BW).

There was no inverse dynamics torque data for strides with inward perturbations. Inward perturbations lead to cross-stepping of the right foot onto the left treadmill, not allowing for inverse dynamics torque calculation [23].

The original 82 reflex gains and offset parameters from [6] were used as a reference model. These parameters were optimized using covariance matrix adaptation evolution strategy (CMA-ES [25]) to have the model walk energy efficiently in a forward dynamics simulation. It was optimized for walking on flat ground without disturbances on the virtual body. For all data-driven versions of the RNM, the same muscle parameters and body geometry were used as in this original [6]; they were not mutable in any (re-)optimization described in the following subsections.

The data-driven model using the original parameters from Song and Geyer [6] is referred to in the remainder of this work as the 'original DDRNM'.

C. Optimized DDRNM

A new set of values for the 82 reflex gains and offsets was found after optimizing the data-driven model. The goal of the optimization was to have normalized modeled output torque of the stance-leg be close to normalized human torques of the stance-leg. This second model is referred to as the 'optimized DDRNM' in the remainder of the text.

The optimization objective was to find a single, constant parameter set θ^* that minimizes the mean weighted absolute normalized torque difference:

$$\theta^* = \underset{\theta}{\operatorname{argmin}} \left\{ \frac{1}{N_j N_t} \sum_{j=1}^{N_j} \sum_{t=1}^{N_t} \frac{|T_{h,j}(t) - T_{m,j}(t,\theta)|}{\sigma_{h,j}(t)} \right\}, \quad (1)$$

in which $T_{h,j}(t)$ is the normalized human joint torque, $T_{m,j}(t,\theta)$ is the normalized model joint torque for a given joint j, reciprocal weighting factor $\sigma_{h,j}(t)$ is the time-dependent standard deviation of normalized torque across subjects, calculated from human data for that joint. The amount of joints

is given by $N_j = 4$ (all joints in the stance leg: hip ab-/adduction, hip flexion/extension, knee flexion/extension and ankle plantar-/dorsiflexion), $t = 1, \ldots, N_t$ is a given discrete time instant, assuming constant time step, where N_t is the amount of data points that cover 16 strides (see Sec II-B).

CMA-ES was used, with a population of 20 samples per generation, evolving over 4,000 generations. The parameter search space was unbounded and initialized with the parameters from the Original DDRNM. To avoid a local optimum, every 400 generations the covariance and related variables were reset to their initial value, while keeping the best solution candidate as the mean. A parallel CMA-ES optimization of 4,000 generations took about 15 hours on a PC with two Xeon E5-2630 V4 CPUs, 2.2 GHz, 20 logical cores with 40 threads [Intel, Santa Clara, USA] running the MATLAB 2016b Simulink version of the model in Accelerator Mode.

D. Optimized Extended DDRNM

When humans counteract anteroposterior perturbations applied at the pelvis directly after right foot toe-off, large modulations occur in the left ankle joint torques [23]. A backward perturbation is counteracted by applying less plantarflexion in the stance leg after perturbation, whereas forward perturbations results in more plantarflexion in the first half of stance, and less before push off. No change in foot placement, w.r.t. the whole body CoM, after anteroposterior perturbations was observed [22], [23]. However, the same studies suggest that for mediolateral perturbations a change in step width and duration are strategies used by humans.

The original RNM was optimized to respond to whole body CoM velocity changes, e.g. due to perturbations, by changing step length [6]. It has a supra-spinal control element that decides foot placement, based on whole body CoM velocity and position with respect to the feet. However, it does not have a specific control module to modulate the muscle excitation of muscles around the ankle in a human-like way in case of perturbations (as is also discussed in Sec. III). Therefore, we propose an extension to the RNM by adding an extra control module (M11) that does excite or inhibit muscles of the stance-foot ankle, based on whole body anteroposterior CoM velocity deviations (see Fig. 2) but does not activate after mediolateral CoM velocity deviations. The possible neurophysiology of M11 is discussed in Sec. IV-A.

Module M11 has an **u**pper ($v_{t,u}$) and **l**ower ($v_{t,l}$) **t**hreshold to detect a whole body CoM velocity deviation (Δv) between the real whole body CoM velocity v and the typical or expected whole body CoM velocity $\hat{v}$. If this deviation crosses a threshold, due to a perturbation, the muscles around the ankle will be excited or inhibited. Muscles acting around the ankle are the Soleus (SOL), Tibialis Anterior (TA) and Gastrocnemius (GAS). The SOL (plantarflexor) and the TA (dorsiflexor) are mono-articular muscles. The GAS is a bi-articular muscle, imposing plantarflexion on the ankle and flexion on the knee. The amount of inhibition or excitation (S_x for each muscle x, i.e. SOL, TA or GAS) is linearly related to the difference between threshold $v_{t,u/l}$ and Δv. Note that there is always neural measurement delay and subsequent neural excitation delay.

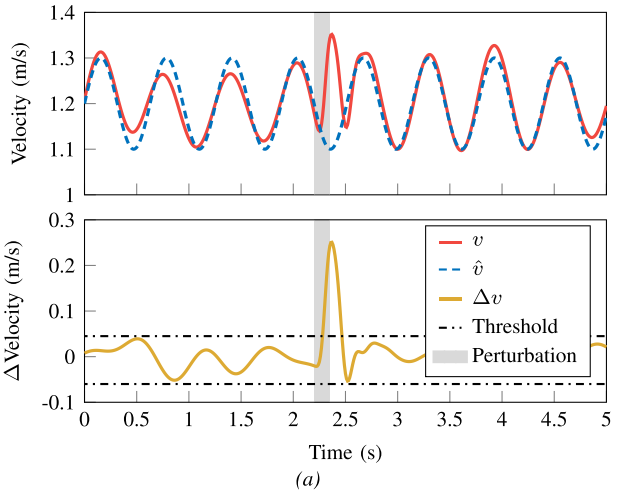

(a)

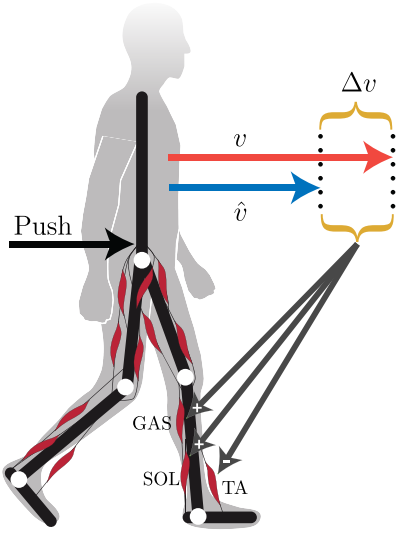

(b)

Fig. 2. (a) Whole body CoM velocity deviation detection uses the real CoM velocity (v), expected CoM velocity ($\hat{v}$) and activates control module M11 based on a threshold on their difference (Δv). Although v barely passes the upper bound of the normal cyclic behavior, the effect of perturbation (shown with shaded area) is directly detected. (b) Schematic overview of how M11 excites/inhibits muscles around the ankle. Representing the scenario of the example in Fig. 2a, Δv passing the *upper* boundary will excite (+) the GAS and SOL of the stance leg and will inhibit (−) the TA.

The time-varying expected whole body CoM velocity $\hat{v}$ was calculated, for each moment in time, as the average of the whole body CoM velocity over five unperturbed strides. The signal of each stride was re-sampled and linearly stretched to synchronize all gait events before averaging.

In summary, for each moment in time (t) the contribution of module M11, at the level of the spine, to the excitation (S) of a muscle x is given by:

$$\Delta v(t) = v(t - \Delta t) - \hat{v}(t - \Delta t) \tag{2}$$

$$S_{x,\mathrm{M11}}(t) = \begin{cases} G_{u,x} \cdot (\Delta v(t) - v_{t,u}), & \text{if } \Delta v(t) > v_{t,u} \\ G_{l,x} \cdot (\Delta v(t) - v_{t,l}), & \text{if } \Delta v(t) < v_{t,l} \\ 0, & \text{otherwise,} \end{cases} \tag{3}$$

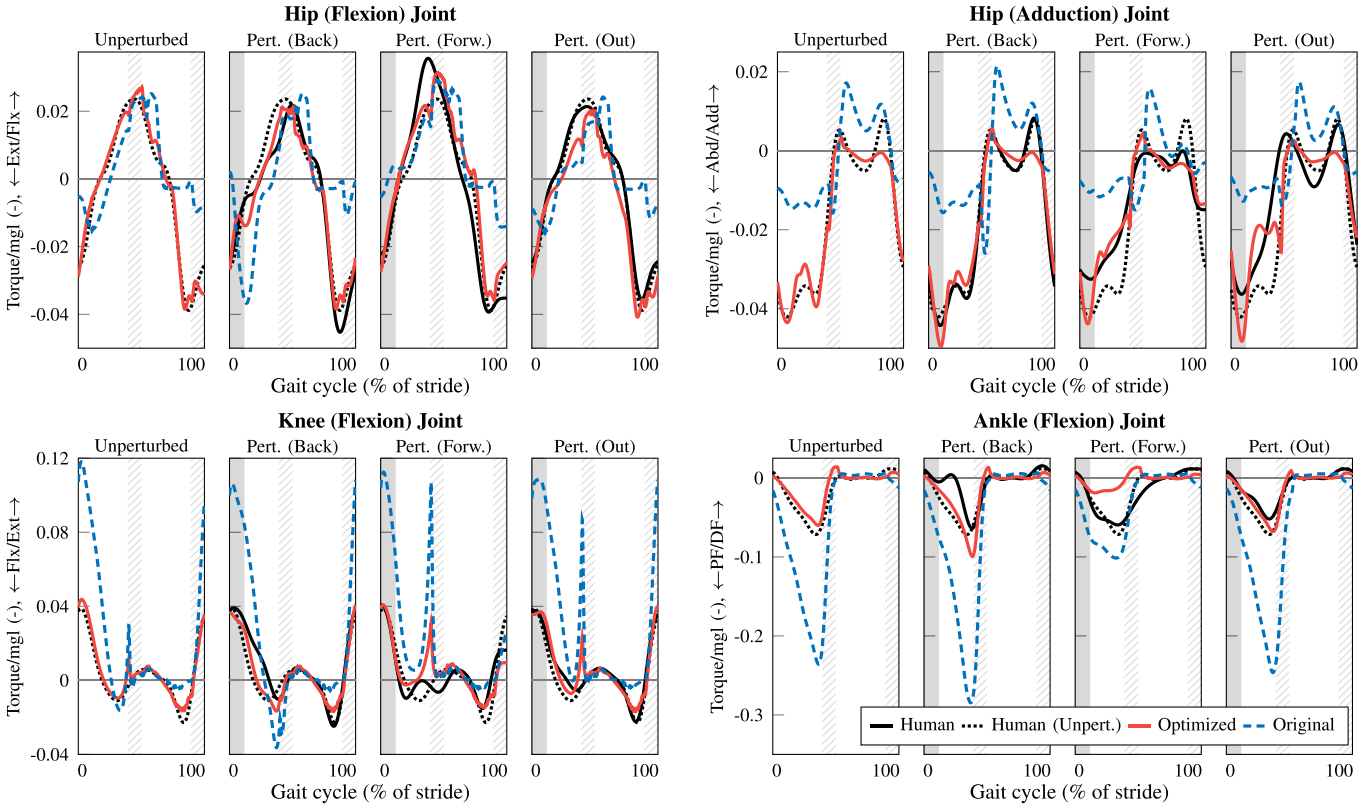

Fig. 3. Normalized human torques compared to predicted torques from the original DDRNM and the optimized DDRNM. Full stride of left leg (initial stance leg) during and after perturbation is shown, which shows most of the counteraction against perturbations. Graph starts at right toe-off at 0%. The solid shaded area indicates when the perturbation was applied, the hatched areas indicate periods of double stance. Four situations are shown to compare unperturbed and perturbed (denoted as 'Pert.') walking for each joint. The human torque pattern for unperturbed walking is repeated in each of the perturbed walking plots for comparison, denoted as 'Human (Unpert.)' in the figure legend. Perturbation direction is with respect to walking direction. Only the highest perturbation magnitude (16% of body weight) is shown.

where $x \in \{\text{SOL,TA,GAS}\}$ indicates the muscle. Module M11 only activates for the leg that is in stance. At the muscle level, these contributions will be delayed w.r.t. the spine, as is done for a all reflex contributions in [3], [6]. A neural measurement delay of the whole body CoM velocity of $\Delta t = 17.5$ ms is used, as this is the same value used for all signals regarding upper body posture from the vestibular organs in [6].

M11 has eight parameters: six linear gains ($G_{\cdot,\cdot}$, two for each muscle) and two thresholds ($v_{t,\cdot}$, the same for all muscles) that are the same for both legs. This model we call the 'optimized extended DDRNM'. This optimized extended DDRNM has $82 + 8 = 90$ parameters, which were all re-optimized in the same manner as explained in Sec. II-C.

III. Results

This section will discuss the torque profiles obtained from the original, optimized and optimized extended versions of the RNM, and compare those to the torques found by inverse dynamics.

A. Original DDRNM

When feeding unperturbed kinematics to the original DDRNM, the resulting normalized torques showed large differences with human data in amplitude and offset (see Fig. 3). The original parameters resulted in peak ankle plantar flexion torques that were 3.3 times higher than human torques. The model hip adduction torque shows a bias when compared to human data. The torques around the knee joint and hip flexion joint showed resemblance in shape, however differences in peak magnitudes can be observed.

Feeding the original DDRNM with data of perturbed walking resulted in a modulation of the ankle torque that is opposite to the ones observed in the experimental data (see Fig. 3). Whereas human subjects showed less plantar flexion torque, in response to a backward perturbation, the model showed more plantar flexion torque. In case of a forward perturbation, humans increased plantar flexion torque in the initial stage after perturbation, while conversely the modeled ankle torque showed substantially less plantar flexion torque.

B. Optimized DDRNM

Optimizing the DDRNM resulted in model torques that resembled the human torques better than using the original parameters (see Table I and Fig. 3). The root mean square error (RMSE) for the optimized DDRNM is lower than the original DDRNM by a factor of 5.2. After optimization, the unbiased zero-lag cross-correlation (R-value), indicating similarity in shape, is higher for all joints except the ankle.

TABLE I
RMSE (NORMALIZED TORQUE) AND R-VALUE OF ORIGINAL DDRNM, OPTIMIZED DDRNM AND OPTIMIZED EXTENDED DDRNM, ALL COMPARED TO HUMAN DATA. COMPARISON OF TORQUE DATA IS DONE PER JOINT IN THE STANCE-LEG, FOR ALL PERTURBATION MAGNITUDES AND DIRECTIONS (I.E. 16 STRIDES) COMBINED

Joint	Original DDRNM: RMSE / R-value	Opt. DDRNM: RMSE / R-value	Opt. Ext. DDRNM: RMSE / R-value
Hip (Flx/Ext)	$1.54{\cdot}10^{-2}$ 0.68	$4.59{\cdot}10^{-3}$ 0.97	$4.60{\cdot}10^{-3}$ 0.97
Hip (Add/Abd)	$1.60{\cdot}10^{-2}$ 0.70	$4.76{\cdot}10^{-3}$ 0.95	$4.73{\cdot}10^{-3}$ 0.95
Knee	$3.12{\cdot}10^{-2}$ 0.85	$5.04{\cdot}10^{-3}$ 0.95	$5.03{\cdot}10^{-3}$ 0.95
Ankle	$7.29{\cdot}10^{-2}$ 0.89	$1.33{\cdot}10^{-2}$ 0.83	$9.13{\cdot}10^{-3}$ 0.93
Overall	$4.12{\cdot}10^{-2}$ -	$7.85{\cdot}10^{-3}$ -	$6.17{\cdot}10^{-3}$ -

After parameter re-optimization, an opposite response in ankle torque modulation after perturbation was still present (see Fig. 3). This indicates that the optimized DDRNM is unable to adjust ankle torques in response to pelvis perturbations in a human-like fashion. Compared to the ankle, the optimized torques of the other joints followed human torque data better for the perturbed cases.

C. Optimized Extended DDRNM

In the optimized extended DDRNM, including M11 resulted in considerable changes in the torque applied at the ankle joint, only when AP perturbations were applied (see Table I and II and Fig. 4). Thus, M11 neither decreased the model's ability to generate human-like torque during normal walking, nor did it change model behavior when ML perturbations were applied. The M11 generated torques closer to human torques for backward perturbed walking and forward perturbed walking (see Fig. 4, and notice decreased RMSE in Table II). The R-value indicates slightly lower similarity to human torque, for the model with M11 for backward perturbations, when compared to the model without M11. However, both correlation values are high. With M11, the model produced more human-like torque responses to a forward perturbation, as reflected by higher correlation (see Table II).

Addition of M11 resulted in more human-like modulation of the muscle excitation in response to an anteroposterior perturbation. For a forward perturbation the optimized DDRNM shows a decreased GAS and SOL excitation and an increase in TA excitation compared to unperturbed walking. This causes a net decrease in plantar flexion torque (see Fig. 5a). In contrast, the optimized extended DDRNM has more excitation of the GAS and SOL and less excitation of TA directly (see Fig. 5b), resulting in torques closer to human torques. For a backward perturbation, the addition of M11 has a large effect on the excitation of the GAS. The optimized DDRNM shows more excitation of the GAS, compared to unperturbed walking,

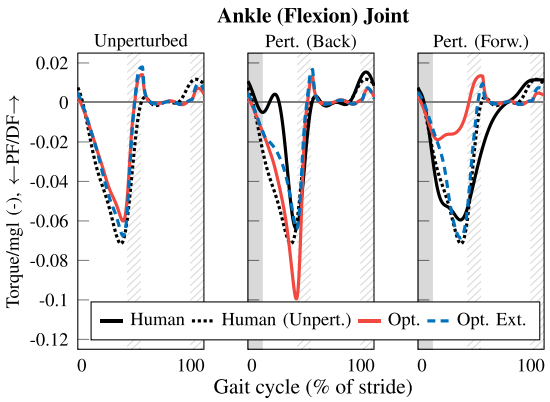

Fig. 4. Normalized human ankle (+dorsiflexion) torque compared to the optimized DDRNM (denoted as 'Opt.') and the optimized extended DDRNM (denoted as 'Opt. Ext.'). Effectively, in the plots in Fig. 3-bottom-right, the original DDRNM is replaced with data from the optimized extended DDRNM. The mediolateral outward perturbation is not evaluated. See Fig. 3 caption for further details.

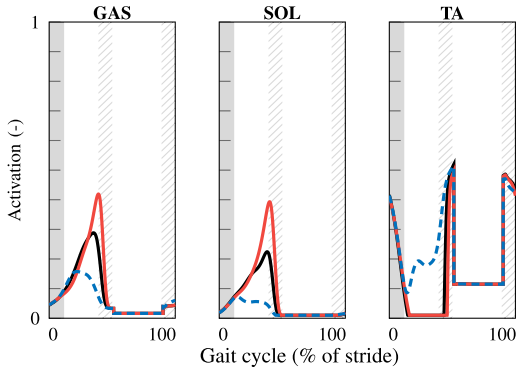

(a) Optimized DDRNM

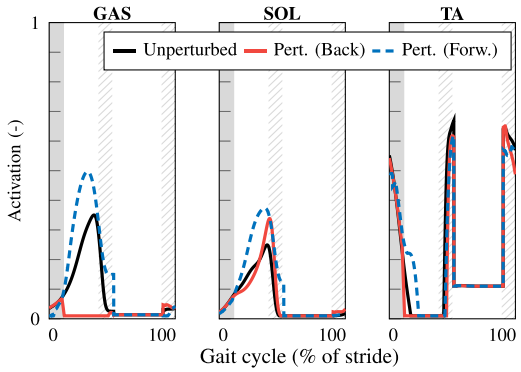

(b) Optimized Extended DDRNM

Fig. 5. Modeled muscle excitation of the GAS, SOL and TA of the stance leg (left leg) in case of applied perturbations for both (a) optimized, and (b) optimized extended DDRNM. Graph starts at right toe-off at 0%. The solid shaded area indicates the perturbation, the hatched areas indicate periods of double stance.

while the optimized extended DDRNM shows less excitation of the GAS.

IV. DISCUSSION

The goal of this work was to investigate whether the original RNM [6] was able to reproduce human kinetics during

TABLE II
RMSE (NORMALIZED TORQUE), SUMMED OVER ALL JOINTS IN THE STANCE LEG, AND R-VALUE OF ORIGINAL DDRNM, OPTIMIZED DDRNM AND OPTIMIZED EXTENDED DDRNM, ALL COMPARED TO HUMAN DATA OF ONE STRIDE FOR PERTURBATIONS OF LARGEST MAGNITUDE (16% BODY WEIGHT) AND AN UNPERTURBED STRIDE

Type	Original DDRNM: RMSE / R-value	Opt. DDRNM: RMSE / R-value	Opt. Ext. DDRNM: RMSE / R-value
Unperturbed	$7.01 \cdot 10^{-2}$ 0.98	$9.32 \cdot 10^{-3}$ 0.96	$8.13 \cdot 10^{-3}$ 0.96
Backward	$9.51 \cdot 10^{-2}$ 0.83	$1.84 \cdot 10^{-2}$ 0.87	$1.17 \cdot 10^{-2}$ 0.84
Forward	$2.61 \cdot 10^{-2}$ 0.87	$2.66 \cdot 10^{-2}$ 0.56	$1.32 \cdot 10^{-2}$ 0.87
Outward	$8.23 \cdot 10^{-2}$ 0.97	$6.95 \cdot 10^{-3}$ 0.98	$6.59 \cdot 10^{-3}$ 0.98

perturbed and unperturbed walking so that it might be used as a controller for P/O devices. When driven by kinematic data, the original DDRNM showed large differences between its predicted torque and torque from measurement data during unperturbed walking. Re-optimization resulted in a good fit for unperturbed walking, but not for perturbed walking. Hence, the model was extended with whole body CoM velocity deviation feedback to excite and inhibit muscles around the ankle. Re-optimization of this extended model's reflex parameters resulted in joint torques closer to human torques for both perturbed and unperturbed walking, shown by lower torque imitation error and higher torque signal correlations. The original DDRNM's generation of plantar flexion torque in case of backward perturbations, which is opposite to the human's response, was no longer present after the model's extension with whole body CoM feedback and re-optimization.

A. Using Whole Body CoM Information for Balance and Its Possible Underlying Neurophysiology

The original RNM from [6] uses whole body CoM position and velocity for step adjustment, but could not use it to modulate torque responses around the ankle. Such stepping strategies have been known from balance control literature, as Hof *et al.* [26] suggested that the body CoM position and velocity seem to be involved in controlling foot placement in response to mediolateral information.

The question remains, however, what the underlying neurophysiology of our proposed M11 could be. Previous studies showed that whole body CoM states encode for muscle activity in response to perturbed balance [27], [28]. Since the CoM states depend on the movement of *all* body segments, consequently information from multiple sensory systems together with an internal model of body dynamics have to be integrated by supraspinal circuits to reconstruct an internal representation of whole body CoM states. Several studies have shown that fusion of visual, vestibular and proprioceptive information is used to control the whole body CoM during standing to maintain balance [29]–[31]. This process of sensory integration can be modelled as an adaptive Kalman filter [32]. The cerebellum is considered to act like a sort of Kalman filter [33], predicting states utilizing internal forward models that are updated by delayed available sensory information.

Another study that hints at the involvement of supra-spinal circuits, like how M11 is now modeled, in modulating the ankle muscles to maintain balance during walking, is an experiment in which individuals received anteroposterior pelvis perturbations while their ankle joints could not contribute to the balance recovery [34]. The latter was realized by physically blocking the ankle joints through a pair of modified ankle-foot orthoses with pin feet. The amplitude of the evoked responses, delayed by around 100 ms, were dependent on the perturbation magnitude and direction, and qualitatively similar to responses when walking without the ankle-foot orthoses. These results imply that ankle muscle responses can be evoked without changes in proprioceptive information of the ankle muscles themselves. This also suggests the involvement of supra-spinal instead of only spinal circuits, which would also be in line with a rather long delay of the responses of around 100 ms.

B. Limitations and Future Work

Driving the model with kinematic data does not allow it to learn how to imitate human foot-step placement in the supraspinal reflex network. Moreover, the optimal controller parameters that produce a human-like torque response to forced kinematic input, might not generate stable walking when applied in a forward dynamics simulation or real-world application where the dynamics close the loop between applied torque and resultant motion. In future work, evaluating cost objectives in both forward and inverse rigid body dynamics simulations, or switching to a direct collocation method [35], might alleviate this problem. However, a reality gap between forward simulation and application on P/O devices will always remain. Therefore, using the DDRNM as a controller is limited to cases as discussed in Sec. I-C where stability is not required (e.g., due to crutch use or because other joints are controlled differently) or when a second type of supervisory controller takes over when the DDRNM torques might result in undesired states.

In this work, we optimized reflex parameters to match joint torques from the stance-leg only, because the stance leg is the one that shows the largest joint torque modulations to counteract the applied perturbations [22]. However, the swing leg also reacts to the applied perturbations, e.g. by additional hip abduction torque when perturbed outward. Although higher torque might hint at outward stepping, this mediolateral stepping response cannot be investigated in full detail from the current results due to the inverse dynamics nature of the DDRNM. In future work, M11 will be extended to also excite/inhibit the contralateral muscles of the swing leg, e.g. those around the contralateral hip and investigate the model's foot placement in both AP and ML directions.

After extending and re-optimizing the model, the DDRNM could capture the direction and approximate magnitude of the human responses, but still some differences with the human torque response remain. The torque match between model and data is lower for perturbed strides compared to unperturbed strides (see Fig. 4, Table I and Table II). The reflexes in M11

were kept simple, having only gain and threshold parameters, in line with the reflexes of the original model [3], [6]. Adding more signals or modules could potentially improve the torque fit, at the risk of over-fitting the model to the data, resulting in responses that generalize poorly. In future work, an optimal balance should be found between increasing the model's complexity (i.e. number of signals or modules) and the quality of the torque reproduction and generalization by promoting low gains or sparsity through regularization during optimization and evaluations in multiple scenarios.

C. RNM as a Controller for P/O Devices

A state-of-the-art review in [2] suggests that active actuation of P/O devices is needed to give patients full support during the entire gait cycle, reduce metabolic cost while walking at a self-selected speed, increase gait symmetry and reduce wear-and-tear of the user's unaffected joints.

The extended DDRNM has potential to be a controller to assist walking, without having to switch between different control modes or gait trajectories. Previous research has already shown the potential of the original RNM in real-world P/O devices in the lab [17], [19], [36], [37] but also in commercially available devices, such as the active Ottobock/BionX emPOWER prosthetic ankle. Future work should show if the proposed robustness claims of using a DDRNM controller also have benefits in activities of daily life when used in lower-extremity exoskeletons.

The extended DDRNM controller requires reliable state information from the P/O device as its input. Estimating whole body CoM states with sufficient accuracy from a single inertial measurement unit (IMU) and joint encoders during stance [38] and estimating whole body CoM state and GRF during walking with three IMUs [39], [40] seem feasible measurement strategies to be able to use the extended DDRNM as a controller outside of a lab environment. In the original [6] and in this work, noise-free signals were used as input to the (DD)RNM, resulting in a model that might not be robust to sensor noise and bias. However, experience from our previous work using IMUs and encoders for active balance control [38] and the fact that muscle dynamics act as a low-pass filter both suggest that performance of a DDRNM controller with real-world sensors would be as expected. Any detrimental effects of noise could also be limited further by adding feed-forward drive [41], e.g. by using Central Pattern Generators (CPGs) in the spinal cord [42]. Negative contributions of sensor bias can be counteracted by continuous or periodic (re)calibration.

Furthermore, the original [6] and extended (DD)RNM model were optimized to walk at a single speed only. In [43] the authors showed that the addition of feed-forward drive through CPGs allows for speed changes. This could extend the number of scenarios to which a DDRNM controller is applicable in P/O devices.

V. Conclusion

This study proposes an extension of the RNM with whole body CoM velocity feedback at the ankle joint to achieve more human-like ankle torque responses to anteroposterior perturbations during walking. With this extension, the model is able to reproduce able-bodied joint torques during unperturbed and anteroposteriorly perturbed walking well. However, the efficacy of the model's anterioposterior ankle torque modulation and mediolateral stepping strategy should both be verified with forward simulation.

For application in the control of P/O devices, using an optimized extended data-driven RNM controller appears to be a promising controller candidate. Measured kinematics from the device would allow a P/O device to mimic able-bodied joint torque responses under both unperturbed and perturbed walking conditions.

Acknowledgment

The authors would like to thank Mark Vlutters for sharing his data and his help with processing.

References

[1] R. J. Farris, H. A. Quintero, S. A. Murray, K. H. Ha, C. Hartigan, and M. Goldfarb, "A preliminary assessment of legged mobility provided by a lower limb exoskeleton for persons with paraplegia," *IEEE Trans. Neural Syst. Rehabil. Eng.*, vol. 22, no. 3, pp. 482–490, May 2014.

[2] M. R. Tucker *et al.*, "Control strategies for active lower extremity prosthetics and orthotics: A review," *J. Neuroeng. Rehabil.*, vol. 12, Jan. 2015, Art. no. 1.

[3] H. Geyer and H. Herr, "A muscle-reflex model that encodes principles of legged mechanics produces human walking dynamics and muscle activities," *IEEE Trans. Neural Syst. Rehabil. Eng.*, vol. 18, no. 3, pp. 263–273, Jun. 2010.

[4] J. M. Wang, S. R. Hamner, S. L. Delp, and V. Koltun, "Optimizing locomotion controllers using biologically-based actuators and objectives," *ACM Trans. Graph.*, vol. 31, no. 4, pp. 1–11, 2012.

[5] T. Geijtenbeek, M. van de Panne, and A. F. van der Stappen, "Flexible muscle-based locomotion for bipedal creatures," *ACM Trans. Graph.*, vol. 32, no. 6, pp. 1–11, Nov. 2013.

[6] S. Song and H. Geyer, "A neural circuitry that emphasizes spinal feedback generates diverse behaviours of human locomotion," *J. Physiol.*, vol. 593, no. 16, pp. 3493–3511, Aug. 2015.

[7] A. V. Hill, "The heat of shortening and the dynamic constants of muscle," *Proc. Roy. Soc. London B, Biol. Sci.*, vol. 126, no. 843, pp. 136–195, 1938.

[8] S. K. Banala, S. H. Kim, S. K. Agrawal, and J. P. Scholz, "Robot assisted gait training with active leg exoskeleton (ALEX)," *IEEE Trans. Neural Syst. Rehabil. Eng.*, vol. 17, no. 1, pp. 2–8, Feb. 2009.

[9] A. Esquenazi, M. Talaty, A. Packel, and M. Saulino, "The ReWalk powered exoskeleton to restore ambulatory function to individuals with thoracic-level motor-complete spinal cord injury," *Amer. J. Phys. Med. Rehabil.*, vol. 91, no. 11, pp. 911–921, 2012.

[10] B. Koopman, E. H. van Asseldonk, and H. van der Kooij, "Speed-dependent reference joint trajectory generation for robotic gait support," *J. Biomech.*, vol. 47, no. 6, pp. 1447–1458, 2014.

[11] S. Wang *et al.*, "Design and control of the MINDWALKER exoskeleton," *IEEE Trans. Neural Syst. Rehabil. Eng.*, vol. 23, no. 2, pp. 277–286, Mar. 2015.

[12] C. Hartigan *et al.*, "Mobility outcomes following five training sessions with a powered exoskeleton," *Topics Spinal Cord Injury Rehabil.*, vol. 21, no. 2, pp. 93–99, 2015.

[13] J. Meuleman, "The design of an assistive robotic gait trainer: LOPES II," Ph.D. dissertation, Dept. Biomech. Eng., Univ. Twente, Enschede, The Netherlands, Nov. 2015.

[14] R. Griffin *et al.*, "Stepping forward with exoskeletons: Team IHMC's design and approach in the 2016 cybathlon," *IEEE Robot. Autom. Mag.*, vol. 24, no. 4, pp. 66–74, Dec. 2017.

[15] T. Vouga, R. Baud, J. Fasola, M. Bouri, and H. Bleuler, "TWIICE—A lightweight lower-limb exoskeleton for complete paraplegics," in *Proc. Int. Conf. Rehabil. Robot. (ICORR)*, Jul. 2017, pp. 1639–1645.

[16] S. O. Schrade *et al.*, "Development of VariLeg, an exoskeleton with variable stiffness actuation: First results and user evaluation from the CYBATHLON 2016," *J. Neuroeng. Rehabil.*, vol. 15, no. 1, pp. 1–18, Dec. 2018.

[17] A. R. Wu *et al.*, "An adaptive neuromuscular controller for assistive lower-limb exoskeletons: A preliminary study on subjects with spinal cord injury," *Frontiers Neurorobot.*, vol. 11, p. 30, Jun. 2017.
[18] F. Tamburella *et al.*, "Neuromuscular controller embedded in a powered ankle exoskeleton: Effects on gait, clinical features and subjective perspective of incomplete spinal cord injured subjects," *IEEE Trans. Neural Syst. Rehabil. Eng.*, vol. 28, no. 5, pp. 1157–1167, May 2020.
[19] C. Meijneke *et al.*, "Symbitron exoskeleton: Design, control, and evaluation of a modular exoskeleton for incomplete and complete spinal cord injured individuals," *IEEE Trans. Neural Syst. Rehabil. Eng.*, vol. 29, pp. 330–339, 2021.
[20] F. Dzeladini *et al.*, "Effects of a neuromuscular controller on a powered ankle exoskeleton during human walking," in *Proc. 6th IEEE Int. Conf. Biomed. Robot. Biomechatronics (BioRob)*, Jun. 2016, pp. 617–622.
[21] S. Song and H. Geyer, "Evaluation of a neuromechanical walking control model using disturbance experiments," *Frontiers Comput. Neurosci.*, vol. 11, p. 15, Mar. 2017.
[22] M. Vlutters, E. H. F. Van Asseldonk, and H. Van der Kooij, "Center of mass velocity based predictions in balance recovery following pelvis perturbations during human walking," *J. Exp. Biol.*, pp. 1514–1523, Jan. 2016.
[23] M. Vlutters, E. H. F. van Asseldonk, and H. van der Kooij, "Lower extremity joint-level responses to pelvis perturbation during human walking," *Sci. Rep.*, vol. 8, no. 1, p. 14621, Dec. 2018.
[24] A. L. Hof, "Scaling gait data to body size," *Gait, Posture*, vol. 3, no. 4, pp. 222–223, 1996.
[25] N. Hansen, "The CMA evolution strategy: A comparing review," in *Towards a New Evolutionary Computation*. Berlin, Germany: Springer, 2006, pp. 75–102.
[26] A. Hof, S. Vermerris, and W. Gjaltema, "Balance responses to lateral perturbations in human treadmill walking," *J. Exp. Biol.*, vol. 213, no. 15, pp. 2655–2664, 2010.
[27] T. D. J. Welch and L. H. Ting, "A feedback model reproduces muscle activity during human postural responses to support-surface translations," *J. Neurophysiol.*, vol. 99, no. 2, pp. 1032–1038, Feb. 2008.
[28] J. H. Pasma, J. van Kordelaar, D. de Kam, V. Weerdesteyn, A. C. Schouten, and H. van der Kooij, "Assessment of the underlying systems involved in standing balance: The additional value of electromyography in system identification and parameter estimation," *J. Neuroeng. Rehabil.*, vol. 14, no. 1, p. 97, Dec. 2017.
[29] R. Peterka, "Sensorimotor integration in human postural control," *J. Neurophysiol.*, vol. 88, no. 3, pp. 1097–1118, 2002.
[30] T. Kiemel, Y. Zhang, and J. J. Jeka, "Identification of neural feedback for upright stance in humans: Stabilization rather than sway minimization," *J. Neurosci.*, vol. 31, no. 42, pp. 15144–15153, Oct. 2011.
[31] T. Mergner, C. Maurer, and R. J. Peterka, "Sensory contributions to the control of stance," in *Sensorimotor Control of Movement and Posture*. Boston, MA, USA: Springer, 2002, pp. 147–152.
[32] H. van der Kooij, R. Jacobs, B. Koopman, and F. van der Helm, "An adaptive model of sensory integration in a dynamic environment applied to human stance control," *Biol. Cybern.*, vol. 84, no. 2, pp. 103–115, Jan. 2001.
[33] H. Tanaka, T. Ishikawa, and S. Kakei, "Neural evidence of the cerebellum as a state predictor," *Cerebellum*, vol. 18, no. 3, pp. 349–371, Jun. 2019.
[34] M. Vlutters, E. H. F. van Asseldonk, and H. van der Kooij, "Ankle muscle responses during perturbed walking with blocked ankle joints," *J. Neurophysiol.*, vol. 121, no. 5, pp. 1711–1717, May 2019.
[35] A. J. Van Den Bogert, D. Blana, and D. Heinrich, "Implicit methods for efficient musculoskeletal simulation and optimal control," *Proc. IUTAM*, vol. 2, pp. 297–316, Jan. 2011.
[36] M. F. Eilenberg, H. Geyer, and H. Herr, "Control of a powered ankle–foot prosthesis based on a neuromuscular model," *IEEE Trans. Neural Syst. Rehabil. Eng.*, vol. 18, no. 2, pp. 164–173, Apr. 2010.
[37] N. Thatte and H. Geyer, "Toward balance recovery with leg prostheses using neuromuscular model control," *IEEE Trans. Biomed. Eng.*, vol. 63, no. 5, pp. 904–913, May 2016.
[38] A. Emmens *et al.*, "Improving the standing balance of paraplegics through the use of a wearable exoskeleton," in *Proc. 7th IEEE Int. Conf. Biomed. Robot. Biomechatronics (Biorob)*, Aug. 2018, pp. 707–712.
[39] M. I. M. Refai, B.-J.-F. van Beijnum, J. H. Buurke, and P. H. Veltink, "Portable gait lab: Tracking relative distances of feet and CoM using three IMUs," *IEEE Trans. Neural Syst. Rehabil. Eng.*, vol. 28, no. 10, pp. 2255–2264, Oct. 2020.
[40] M. I. M. Refai, B.-J.-F. van Beijnum, J. H. Buurke, and P. H. Veltink, "Portable gait lab: Estimating 3D GRF using a pelvis IMU in a foot IMU defined frame," *IEEE Trans. Neural Syst. Rehabil. Eng.*, vol. 28, no. 6, pp. 1308–1316, Jun. 2020.
[41] T. J. Brug, F. Dzeladini, A. R. Wu, and A. J. Ijspeert, "Combining a 3D reflex based neuromuscular model with a state estimator based on central pattern generators," in *Converging Clinical and Engineering Research on Neurorehabilitation II* (Biosystems & Biorobotics), vol. 15. Cham, Switzerland: Springer, 2017, pp. 633–637.
[42] A. J. Ijspeert, "Central pattern generators for locomotion control in animals and robots: A review," *Neural Netw.*, vol. 21, no. 4, pp. 642–653, 2008.
[43] F. Dzeladini, J. van den Kieboom, and A. Ijspeert, "The contribution of a central pattern generator in a reflex-based neuromuscular model," *Frontiers Hum. Neurosci.*, vol. 8, pp. 1–18, Jun. 2014.